Dip-dependent spreading correction through prestack migration/inversion

Børge Amtsen and Anders Sollid, *Statoil, Norway* **PP2.6**

SUMMARY

Fazzari (1992)showed that the conventional geometrical spreading correction used in seismic processing is incorrect for dipping beds at large traveltimes. This can be remedied by using a dip-dependent geometrical spreading correction, as was demonstrated by Fazzari. We show that it is also possible to provide exactly the same spherical spreading correction via prestack migration by modifying existing schemes slightly. This modification is derived via a least-squares inverse scheme relating seismic data to reflection coefficients. The scheme also works for poststack data, but would require the use of a true zero-offset model for migration instead of the standard exploding reflector model. For illustration two simple data examples are provided. In the first example 3-D prestack migration schemes are used to image two point-diffractors. The conventional schemes grossly underestimates the strength of the diffractors. A modified scheme is shown to provide a much more correct amplitude. The data for the second example consists of a single split-spread record shot over a steeply dipping reflector. The results of conventional and modified 2-D prestack schemes are compared, and the modified scheme is shown to provide better estimates of the reflection coefficient.

INTRODUCTION

Migration methods based on the wave equation have been in practical use as a tool for processing and interpretation of seismic data since the early 1970's (Claerbout 71). In the years following substantial practical experience has been gained by the seismic industry on how to handle migration in various situations. The use of migration has undoubtly led to improved quality of interpreted geological models. With the 1980's came the introduction of linearized inversion schemes (Clayton and Stolt 81, Stolt and Weglein 85)) (and even comprehensive non-linear schemes (Tarantola 84)), where the aim was to get a detailed map of wave velocities and densities of the subsurface with prestack data as input. Few of these schemes have gained wide acceptance in the industry, mainly because they are thought to be little less than an academic rephrasing of well known migration algorithms. In some respects this is true, particularly if viewed as a structural imaging tool. However, if properly interpreted, inversion schemes can be used to get a better understanding of how migration handles amplitude information, especially with regards to reflection coefficients and propagation effects such as geometrical spreading losses. With the widespread use of work stations and high-quality color displays, interpreters can easily make amplitude attribute maps from processed seismic data. These maps are often used to infer information about rock properties such as porosity and fluid contents.

It is essential that these maps really reflect true properties of the sub-surface and not merely an artifact from the imaging method being used. We show how one aspect of preserving amplitude information, namely dip-dependent geometrical spreading (Fazzari 92)can be easily included in 3-D prestack and poststack migration schemes.

THEORY

Forward problem

Our forward model consists of an acoustic medium where the density is constant and a smooth background velocity c_0 is assumed to be known. The true, unknown velocity c at position $\boldsymbol{x}$ is close to the background model in the sense that

$$\frac{c(\boldsymbol{x}) - c_0(\boldsymbol{x})}{c_0(\boldsymbol{x})} \ll 1 . \quad (1)$$

The difference $\delta\tilde{p}$ between the acoustic pressure p_0 in the background model and the pressure p related with the unknown velocity c can be expressed by the equation

$$\delta\tilde{p}(\boldsymbol{x}_0,\omega) = - \int dV(\boldsymbol{x})\, g(\boldsymbol{x},\omega;\boldsymbol{x}_0) p_0(\boldsymbol{x},\omega)\alpha(\boldsymbol{x}). \quad (2)$$

Here w is the frequency and $g(\boldsymbol{x}, \text{w}; \boldsymbol{x}_0)$ is the Green's function in the background model. α is given by

$$\alpha(x) = \frac{\omega^2}{c_0^2(\boldsymbol{x})}\left[1 - \frac{c_0^2(\boldsymbol{x})}{c^2(\boldsymbol{x})}\right] . \quad (3)$$

a is related to the acoustic reflection coefficient R via the relation (Stolt and Weglein 85)

$$\partial_n \alpha(\boldsymbol{x}) \approx - \frac{\omega^2}{c_0^2(\boldsymbol{x})} cos^2(\theta) R(\boldsymbol{x},\theta). \quad (4)$$

Here, the angle θ is half the angle between incident and reflected waves at position x, and the partial derivative ∂_n is normal to the local dip. The pressure in the background model is given by

$$p_0(\boldsymbol{x},\omega) = \int dV(\boldsymbol{x}_0)\, g(\boldsymbol{x}_0,\omega;\boldsymbol{x}) p_0(\boldsymbol{x}_0,\omega) s(\omega,\boldsymbol{x}_0), \quad (5)$$

where s is the source distribution.

Inverse problem

We define the inverse problem as minimizing the error function J with respect to α

$$J = \int d\omega \int dV(\boldsymbol{x}_0) [\delta p(\boldsymbol{x}_0,\omega) - \delta\tilde{p}(\boldsymbol{x}_0,\omega)]^2, \quad (6)$$

where $\delta p(\boldsymbol{x}_0$, w) is the observed data computed from the seismic data at the surface by

$$\delta p(\boldsymbol{x}_0, \omega) = \int dS \partial_n \tilde{g}(\boldsymbol{x}_r, \omega; \boldsymbol{x}_0) \delta p(\boldsymbol{x}_r, \omega). \tag{7}$$

Here $\tilde{g}$ is the adjoint Green's function. The surface integral extends over all receiver coordinates and ∂_n denotes differentiation with respect to the surface normal. The left hand side of equation (7) is simply the downward extrapolated data at position $\boldsymbol{x}_0$ in the subsurface. The error in equation (6) is in principle minimized over the space spanned by all frequencies and the complete subsurface volume to be imaged. Equation (6) has a well-known solution of the form

$$\boldsymbol{\alpha} = \left(\boldsymbol{F}^T \boldsymbol{F}\right)^{-1} \boldsymbol{F}^T \delta \boldsymbol{p} \tag{8}$$

where $\delta \boldsymbol{p}$ is the migrated data written in vector form, and $\boldsymbol{\alpha}$ is the unknown function a written in vector form. The superscript T denotes transponation and complex conjugation. The inverse of the matrix $\boldsymbol{F}^T \boldsymbol{F}$ can not be easily calculated, instead we use the diagonal elements only to arrive at the approximate inverse

$$\boldsymbol{F}^T \boldsymbol{F} \approx \int d\omega \int dV(\boldsymbol{x}_0) [g(\boldsymbol{x}, \omega; \boldsymbol{x}_0) p_0(\boldsymbol{x}, \omega)]^* g(\boldsymbol{x}, \omega; \boldsymbol{x}_0) p_0(\boldsymbol{x}_0, \omega).$$

This leads to the following expression for a

$$\alpha(\boldsymbol{x}) = \frac{\int d\omega \int dV(\boldsymbol{x}_0) [g(\boldsymbol{x}, \omega; \boldsymbol{x}_0) p_0(\boldsymbol{x}, \omega)]^* \delta p(\boldsymbol{x}_0, \omega)}{\int d\omega \int dV(\boldsymbol{x}_0) [g(\boldsymbol{x}, \omega; \boldsymbol{x}_0) p_0(\boldsymbol{x}, \omega)]^* g(\boldsymbol{x}, \omega; \boldsymbol{x}_0) p_0(\boldsymbol{x}_0, \omega)}.$$

Invoking the high-frequency asymptotic approximations for the Greens' function $\boldsymbol{g}$ and the migrated data $\delta \boldsymbol{p}$, equation (9) reduces to:

$$\alpha(\boldsymbol{x}) = \frac{\int d\omega\, p_0^*(\boldsymbol{x}, \omega) \delta p(\boldsymbol{x}, \omega)}{\int d\omega\, p_0^*(\boldsymbol{x}, \omega) p_0(\boldsymbol{x}, \omega)}. \tag{9}$$

Equation (9) is nothing else than Claerbout's U/D imaging principle for pres t ack migration, derived from least -squares inverse theory. The left hand side now has a physical meaning, relating the migration image to the local reflection coefficient through equation (4). Usually equation (9) is approximated with

$$\alpha(\boldsymbol{x}) \approx \int d\omega\, p_0^*(\boldsymbol{x}, \omega) \delta p(\boldsymbol{x}_0, \omega). \tag{10}$$

Two interesting conclusions can be drawn from equations (9) and (IO). First, prestack migration via equation (9) provides an estimate of a quantity closely related to the local reflection coefficient. Second, equation (9) provides the correct correction for geometrical spreading losses, while the approximate form equation (10) fails to do so. The main shortcoming of equation (10) compared to (9) is the lack of compensation for geometrical spreading along the raypath from the source to the receiver. This is taken into account in equation (9) through the denominator term involving the forward modeled data p_0. In effect equation (10) fails to take into account and correct for the geometrical spreading from the source down to the reflection point. Equation (10) corresponds to conventional prestcak migration while equation (9) represents a less used modified scheme. For cases where amplitude preservation is important, equation (9) should be used in favor of (10).

Equation (9) was originally developed for prestack data. It is however possible to use this equation also for poststack migration. However, one would have to abandon the much used exploding reflector model and instead use a true zero-offset model implied by equation (9).

DATA EXAMPLE

Fazzari (1992) have pointed out that conventional poststack migration fails to provide the correct compensation for geometrical spreading. Essentially migration only provides half the correction, only compensating for the geometrical spreading from the point of reflection and upwards to the receivers. However, the geometrical spreading from the source and down to the reflection point still remains. Conventional correction techniques, fails to provide the needed correction, because it is based on the plane-layer assumption. Reflections from dipping beds are incorrectly compensated. Fazzari (1992) showed that this effect may lead to incorrect amplitudes for strongly dipping reflections. To provide the correct compensation, Fazzari (1992) proposed to use a dip-dependent correction. By using the expression for prestack migration given in equation (9), we show that prestack migration automatically provide the correct compensation for geometrical spreading. It is however also true that prestack migration based on equation (10) provides the wrong compensation for geometrical spreading. The main difference between equation (9) and equation (10) is that the denominator in the former contains the forward modelled wavefield associated with the background model. This factor is missing in equation (10). Equation (10) (or closely related forms) is conventionally used for prestack migration.

Diffractor model

To illustrate the effect of geometrical spreading compensation, we use a model consisting of a constant background velocity equal to 3000 m/s with two point diffractors embedded at a depth of 600 m and 1200 m respectively. The strengths of the two diffractors are equal. Figure 1 shows the result of 3-D prestack migration of data obtained with a single shot in the middle of the model. The conventional approach given by equation (10) was used to create the image. The lower point diffractor has a significantly lower amplitude than the upper reflector and is in fact invisible without scaling. Figure 2 shows 3-D prestack migration based on equation (9). The amplitude of the lower diffractor is much larger than on Figure 1. In principle the amplitude of the upper and lower amplitude should have been equal, but the limited aperture used in the example leads to amplitude losses in addition to geometrical spreading. Figure 2 shows anyway a more correct amplitude of the lower diffractor than Figure 1.

Steep-dip model

Figure 3 shows the velocity model used in our next example. Figure 4 shows a prestack migration of a single shot using the conventional equation (10). The amplitude of the strongly dipping reflector starting at a depth of 1 km in the upper right hand corner is strongly underestimated relative to the other reflectors in the image, which is clearly seen by comparing Figure 4 with Figure 5. Figure 5 shows the result of a prestack migration using equation (9). It is clear that the prestack method given by equation (9) gives a much more correct result with respect to amplitudes in the migrated image than the more conventional method given by equation (10). The geometrical spreading for the event travelling from the source to the strongly dipping reflector at a depth of 1 km and back to the receiver array is different than the geometrical spreading for an event travelling from the source and clown to the reflector at 3 km. This is due to the larger velocities along the latter raypath, even though the traveltimes are comparable. Correcting for geometrical spreading before migration would not solve the problem, but instead lead to overcorrection of the strongly dipping reflector, as shown by Fazzari (1992).

CONCLUSIONS

It has been demonstrated that dip-dependent geometrical spreading correction can be built into prestack migration schemes by modifying existing schemes slightly. The equation can be easily derived from least-squares inverse theory, which provides the link between reflection coefficients (medium parameters) and migrated data. Numerical examples have been given for illustration.

References

Claerbout, J. F., 1971, Toward a unified theory of reflector mapping: Geophysics, **36**,467-481.

Clayton, R. W., and Stolt, R. H., 1981, A Born-WKBJ inversion method for acoustic reflection data: Geophysics, **46**,1559-1567.

Fazzari, F., 1992, Dip-dependent divergence correction:, *in* 62nd Ann. Internat. Mtg., Soc. Expl. Geophys., Expanded Abstracts, 1275-1278.

Stolt, R. H., and Weglein, A. B., 1985, Migration and inversion of seismic data: 'Geophysics, **50**,2458-2472.

Tarantola, A., 1984, Inversion of seismic reflection data in the acoustic approximation: Geophysics, **49**,1259-1266.

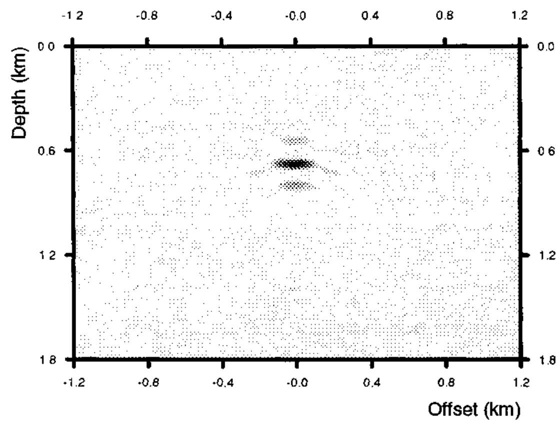

Fig 1. 3-D conventional prestack migration.

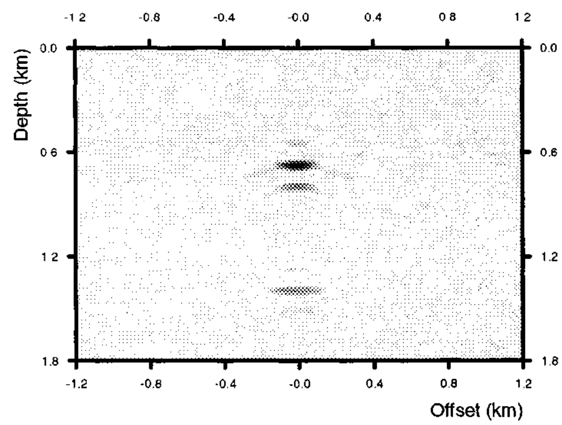

Fig 2. 3-D modified prestack migration.

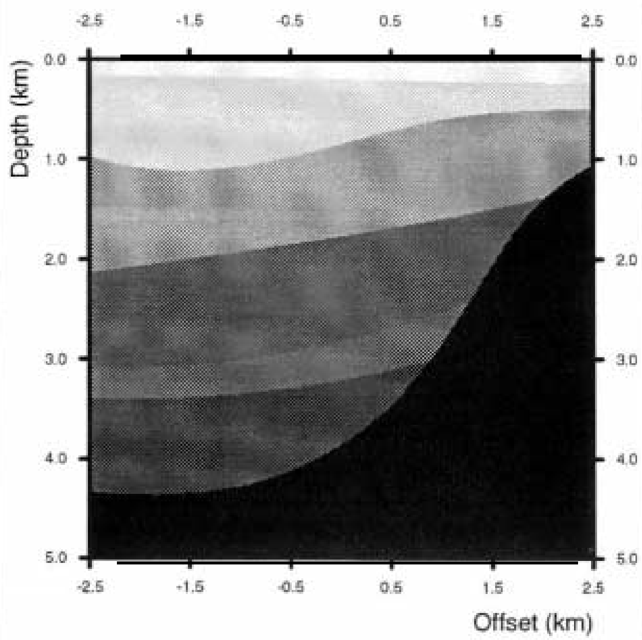

Fig 3. Steep-dip velocity model.

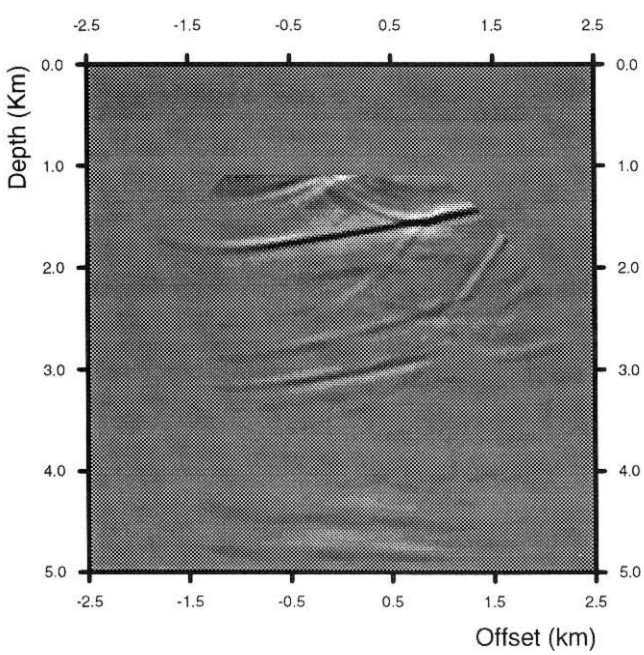

Fig 4. Conventional 2-D prestack migration

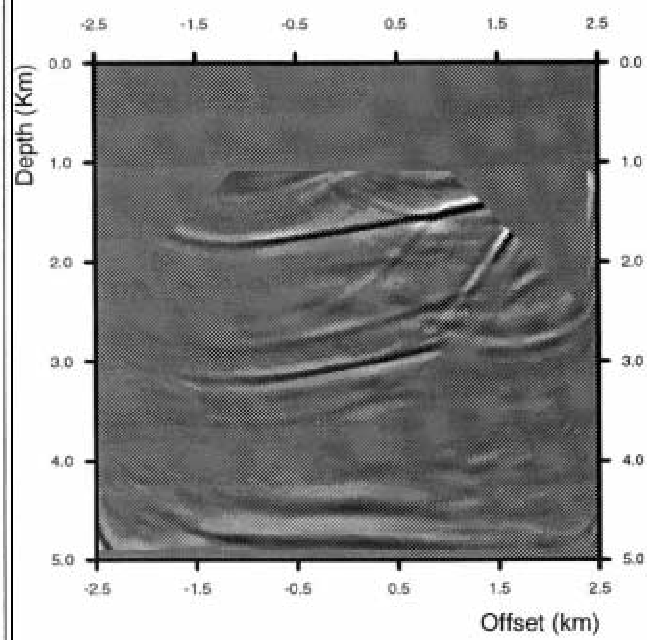

Fig 5. Modified 2-D prestack migration.